JPET Fast Forward. Published on January 14, 2009 as DOI: 10.1124/jpet.108.149989

JPET #149989

Coupling of β2-adrenoceptors to XLαs and Gαs: A new insight into ligand-induced G protein activation

A.I. Kaya, Ö. Uğur, Ş.S. Öner[1], M. Bastepe, H.O. Onaran

Ankara University Biotechnology Institute, Tandogan, Ankara, Turkey (AIK). Ankara University Faculty of Medicine Dept. Pharmacology and Clinical Pharmacology and (AIK, ÖU, ŞSÖ, HOO) Molecular Biology and Technology Development Unit, Sıhhiye, Ankara, Turkey (HOO). Endocrine Unit, Dept. Medicine, Massachusetts General Hospital and Harvard Medical School, Boston, MA, USA (MB)

JPET #149989

Running Title: β2-adrenoceptor-XLαs coupling

Address correspondence to H. Ongun Onaran, Ankara Üniversitesi Tıp Fakültesi, Farmakoloji ve Klinik Farmakoloji Ab.D. Sıhhiye 06100 Ankara, Turkey. Phone: +90 312 311 8829, Fax: +90 312 310 6268, e-mail: onaran@medicine.ankara.edu.tr

Number of Text Pages: 33

Number of Tables:..... 1

Number of Figures: 6

Number of References: 32

Number of Words in Abstract: 227

Number of Words in Introduction: 743

Number of Words in Discussion: 1500

Abbreviations:

βAR: β2-adrenoceptor; XLαs: Extra Large Gαs.

Recommended Section: Cellular and Molecular

ABSTRACT

Gαs and XLαs (Extra-Large Gαs) can both transduce receptor activation into intracellular cAMP generation. It is unknown, however, whether these two *GNAS*-locus products display distinct properties with respect to receptor coupling. Here we show that XLαs couples to the β2-adrenoceptor more efficiently than Gαs. In transfected HEK293 cells and mouse embryonic fibroblasts null for both Gαs and XLαs (2B2 cells), basal cAMP accumulation mediated by XLαs was higher than that mediated by Gαs. Inverse agonist treatment reduced Gαs-mediated basal activity, whereas its effect was markedly blunted on XLαs-mediated basal activity. Rank order of ligand efficacies regarding cAMP accumulation was the same when the receptor was coupled to XLαs or Gαs. However, ligand-induced and XLαs-mediated cAMP generation was higher than that mediated by Gαs. The relatively high efficiency of XLαs-mediated cAMP generation was conditional, disappearing with increased level of receptor expression or increased efficacy of ligand. Full agonist responses in XLαs and Gαs expressing cells were comparable even at low receptor levels, whereas partial agonist responses became comparable only when the receptor expression was increased (>3 pmol/mg). Radioligand binding studies showed that the high affinity component in agonist binding to β2-adrenoceptor was more pronounced in cells expressing XLαs than those expressing Gαs. We discuss these findings in the framework of current receptor-G protein activation models and offer an extended ternary complex model that can fully explain our observations.

INTRODUCTION

Heterotrimeric G proteins, consisting of α, β and γ subunits, constitute a large family of signaling proteins that transmit receptor signals to intracellular effectors. Upon interaction with an active receptor, G proteins undergo a conformational change that results in guanine-nucleotide exchange on the α subunit and dissociation of α and βγ subunits. Dissociated subunits interact with intracellular effectors to modulate their activity. Among others, Gs protein has specifically evolved to transmit receptor signals to the stimulation of adenylyl cyclase that leads to intracellular generation of the second messenger cAMP (see Gilman, 1987; Hamm, 1998 for review).

Alpha subunits of Gs are encoded by the complex *GNAS* locus on the chromosome 20q13 (Kozasa et al., 1988). This locus generates multiple products through the splicing of different alternative first exons onto a common downstream exon (exon 2). Additionally, alternative splicing of exon 3 of Gαs gene results in long and short forms of Gαs protein (Bray et al., 1986). A recently identified product of the *GNAS* locus is the Extra Large αs (XLαs) protein, in which the first exon of Gαs is replaced by the XL-exon that encodes, in rat, 347 instead of 47 amino acids in the amino terminus of Gαs (Kehlenbach et al., 1994). In contrast to Gαs, which is expressed ubiquitously, XLαs is expressed particularly in neuroendrocrine tissues (Pasolli et al., 2000) and derived from the paternal allele (Hayward et al., 1998). Polymorphisms affecting the XL-exon have been shown to be associated with prolonged trauma-induced bleeding in humans (Freson et al., 2001). Additionally, XLαs knockout mice have shown poor postnatal growth and survival, suggesting an important role for XLαs in postnatal development and adaptation (Plagge et al., 2004). Perinatal defects similar to those in XLαs knockout mice have also been identified in two unrelated children who carried large deletions that comprised the paternal *GNAS* allele (Geneviève et al., 2005).

JPET Fast Forward. Published on January 14, 2009 as DOI: 10.1124/jpet.108.149989
This article has not been copyedited and formatted. The final version may differ from this version.

XLαs has been shown to interact with Gβγ dimers to form a stable heterotrimeric complex, and to undergo cholera toxin-induced ADP-ribosylation. It is activated by GTPγS, and upon binding of GTPγS, undergoes a conformational change similar to Gαs (Klemke et al., 2000). It has also been shown that XLαs couples agonist stimulation of different types of Gαs-coupled receptors to the activation of adenylyl cyclase in transfected cells (Bastepe et al., 2002; Linglart et al. 2006). Finally, the point mutation Q548L in XLαs (equivalent to Q227L in Gαs) results in constitutive adenylyl cyclase stimulation (Klemke et al., 2000). Thus, consistent with the fact that XLαs and Gαs share identical functional domains (except their N-terminus), XLαs demonstrates Gαs-like properties. Although there have been conflicting reports about its intracellular distribution, the fact that it couples membrane receptors to adenylyl cyclase strongly suggests that XLαs, like Gαs, is also expressed in the plasma membrane (Kehlenbach et al., 1994; Pasolli et al., 2000; Uğur and Jones, 2000; Linglart et al. 2006). However**,** little is known about the signaling properties of XLαs compared to Gαs. Despite the functional similarities between XLαs and Gαs, their coupling properties to the membrane receptors may diverge due to the difference in their N-termini, which has been implicated to be involved in receptor interaction and activation (Fanelli et al., 1999). Apparently, this difference does not result in receptor selectivity, as all the Gs-coupled receptors investigated to date have also been found to be able to couple to XLαs (Bastepe et al., 2002; Linglart et al. 2006). However, the difference between the two proteins may be particularly important in terms of agonist-directed signal trafficking, where different ligands can couple the same receptor to different G proteins with diverging efficacies. In other words, a set of ligands may exhibit different order of efficacy depending on whether a particular receptor is coupled to Gαs or XLαs, which may have a potential pharmacological importance.

JPET Fast Forward. Published on January 14, 2009 as DOI: 10.1124/jpet.108.149989
This article has not been copyedited and formatted. The final version may differ from this version.

In the present study, we therefore investigated signaling properties of XLαs in comparison with $G\alpha s_L$ (Gαs long form), by measuring its ability to mediate receptor and ligand dependent or independent activation of adenylyl cyclase. We used human β2-adrenoceptor (βAR) as a prototypical Gs-coupled experimental model. The purpose of the present study was two-fold: First, to compare the coupling properties of XLas and Gas to βAR, and second, to gain further insights into the mechanism of G protein-mediated signaling by using a system in which the same receptor is coupled to two different G proteins as a tool. The latter point is discussed in the framework of the current interpretation of the ternary complex models.

JPET Fast Forward. Published on January 14, 2009 as DOI: 10.1124/jpet.108.149989
This article has not been copyedited and formatted. The final version may differ from this version.

METHODS

Cell Culture:

HEK293 cells were grown in DMEM supplemented with penicillin (100u/ml), streptomycin (100µg/ml) and 10% fetal bovine serum (FBS) in a humidified atmosphere of 5% CO_2 at 37 °C. In the case of 2B2 *Gnas* $^{E2-/E2-}$ fibroblasts, where 2nd exon of Gαs or XLαs was disrupted out, DMEM-F12 medium supplemented with 5% FBS was used and cells were grown at 33 ^{o}C.

Plasmid constructs and transfections:

The point mutation (L519P) present in the original cDNA of XLαs was corrected by replacing the P codon with the L codon at the relevant position by standard site directed mutagenesis techniques on the pcDNA3.1(+) vector (Kehlenbach et al., 1995). cDNAs encoding rat XLαs or rat $G\alpha s_L$ were cleaved from the original vectors and re-inserted into pcDNA3.1-hygromycin plasmids. cDNA encoding human βAR was inserted into the pcDNA3.1-zeocin plasmid. HEK293 cells and 2B2 cells were transfected with calcium-phosphate precipitation (Kingston et al., 1996) and DEAE-Dextran methods (Gulick, 1997), respectively. Stable mono-clones were selected using appropriate antibiotics. Protein expression levels of the selected clones or transiently transfected cells were determined by radioligand binding or western blot analysis. HEK293 clones that overexpress βAR at a level of 30 pmol/mg membrane protein were a kind gift of Dr. Tommaso Costa (Istituto Superiore di Sanitá, Rome, Italy). Original cDNAs for human-β_2AR, rat-$G\alpha s_L$ and rat-XLαs were kind gifts of T. Costa (Rome, Italy), TLZ Jones (Washington DC, USA) and WB Huttner (Heildelberg & Dresden, Germany), respectively.

Immunoblots and SDS-PAGE:

Proteins were separated by SDS-PAGE and transferred to PVDF membrane (Biorad, Hercules, CA) by using standard procedures. Proteins were detected by custom-designed polyclonal antibody (produced by Pacific Immunology Corp, CA) raised against the C-terminal decapeptide (NH_2-(Cys)-Arg-Met-His-Leu-Arg-Gln-Tyr-Glu-Leu-Leu) of Gαs (and XLαs), and ECL as described by the manufacturer (Santa Cruz Biotechnology, CA). Densitometric analysis of blots was carried out by using an image analysis system (Raytest, Diana v1.6, Aida v2.43, Straubenhardt, Germany).

Membrane preparations and Receptor binding assays:

Cells were pelleted at 200 g for 5 min at room temperature, resuspended in homogenization buffer (5 mM Tris-HCl pH 7.4, protease inhibitor mixture (Roche Diagnostics, Mannheim, Germany)), and homogenized by passing the suspension (10-15 times) through a 26G syringe tip on ice. The homogenate was centrifuged at 450 x g for 10 min at 4ºC, and the resulting supernatant at 100,000 x g for 30 min at 4ºC (Beckman Coulter Optima LE-80K Ultracentrifuge, CA). The pellet was resuspended in a buffer containing 50 mM Tris-HCl (pH 7.4), DTT 0.3 mg/ml, 5 mM $MgCl_2$, protease inhibitor mixture, and re-pelleted by centrifugation at 100,000 x g for 30 min at 4ºC. The final pellet was suspended in 50 mM Tris-HCl (pH 7.4), 10 mM $MgCl_2$, protease inhibitor mixture, and 25% sucrose at a protein concentration of approximately 2 mg/ml, and stored at -80°C.

In saturation binding assays, 0.5-1 µg membrane protein was incubated with [125I]-iodocyanopindolol (100000 dpm/well) in a total volume of 100 µl buffer (100mM KCl, 10 mM MgCl2, 50 mM Tris-HCl pH 7.4) for 2 hour at 37^{o}C in 96-well plates. The reaction was stopped by rapid filtration through a Whatman GFB glass fiber filter by using a cell harvester

JPET Fast Forward. Published on January 14, 2009 as DOI: 10.1124/jpet.108.149989
This article has not been copyedited and formatted. The final version may differ from this version.

(Skatron Instruments, Lier, Norway). Radioactivity on the filters was counted by using a scintillation counter (Wallac MicroBeta 1450 Trilux, Turku, Finland). Nonspecific binding was determined in the presence of 1 μM cyanopindolol. Competition binding assays were conducted similarly except that varying concentrations of indicated competitor ligands and 20000 cpm/well of [125I]-iodocyanopindolol were used in the presence or absence of GTPγS (1μM) or GPD (100μM) + AlF (20μM NaCl / NaF 10mM) at a final buffer volume of 200 μl. Nucleotide-induced shift in agonist binding curves was found to be more complete with GDP+AlF than with GTPγS. Therefore, we presented the results of the experiments where GDP+AlF were used. Binding curves were analyzed by nonlinear regression of a 4-parameter logistic equation or numerical solution of multisite binding equation in the presence of multiple ligands by means of an in-house MSExcel routine. Binding curves obtained in parallel experiments in the presence or absence of guanine nucleotide were analyzed by sharing receptor concentration and affinity values among binding curves. The effect of parameter sharing was tested by using F statistics.

Determination cAMP accumulation:

Cells were seeded in 96-well plates at a density of 5-10 x 10^3 cells/well 24 hours before the experiment. Two hours before the assay, cells were washed once with serum-free DMEM. Assays were conducted in a total volume of 100 μl at 37 ºC for 5 min. After incubating the cells with the receptor ligands for 5 min at room temperature, cAMP assay was initiated by adding 1 mM isobutylmethylxanthine and terminated by adding 100 μl 0.2 N HCl. cAMP accumulation was determined by a radioimmunoassay as described before (Uğur and Onaran, 1997).

Immunocytochemistry and Confocal microscopy:

Cells, grown on glass cover slips, were washed 3 times with phosphate buffered saline (PBS) and fixed with 2% paraformaldehyde (wt/vol) in PBS for 20 min. After permeabilization with 0.1% Triton X-100 in PBS (vol/vol) for 15 min and blocking for 15 min with 1% bovine serum albumin in PBS (wt/vol), cells were incubated with an antibody raised against carboxyl terminus decapeptide of Gαs (see immunoblotting section above for the specification of the antibody) at a dilution of 1:500 for 1 hour, washed with PBS and then incubated with Cy3 conjugated anti-rabbit antibody (1:1000) (Zymax, CA) for 1 hour at room temperature. Cells were then washed 3 times with PBS and once with distilled water, mounted with Immu-Mount reagent (Shandon, Pittsburgh, PA) and visualized by the use of a confocal microscope (Leica LSM5, Germany).

Modeling and numerical simulations

In order to explain the experimental observations on a quantitative basis we used a modified ternary complex model as schematized in figure 1. In the classical ternary complex models the G protein activation has been considered implicitly as equivalent to the amount of receptor-G protein complex formed, regardless of whether the receptor activation is considered explicitly or not. In the present case however, the G protein activation is considered explicitly as a binary process. Thus, the model given in figure 1 is a new interpretation of the well-known ternary complex model which has been widely used to explain ligand behavior in different contexts. The reason for such a modification is discussed in the discussion section.

In the present scheme, three unconditional affinity constants K, M and L govern ligand-receptor binding, receptor-G protein binding and state transition of the G protein, respectively. Three allosteric constants, α, β and γ, depict the coupling between the following processes: 1)

JPET Fast Forward. Published on January 14, 2009 as DOI: 10.1124/jpet.108.149989
This article has not been copyedited and formatted. The final version may differ from this version.

ligand binding to the receptor and receptor binding to the G protein (α), 2) receptor binding to G protein and G protein activation (β), and 3) ligand binding to receptor-G protein complex and G protein activation (γ). See the left panel of figure 1 for a schematic presentation of the affinity and allosteric constants. All these constants can be defined as follows:

$$K = \frac{[HR]}{[R][H]} \qquad M = \frac{[RG]}{[R][G]} \qquad L = \frac{[G*]}{[G]}$$

$$\alpha K = \frac{[HRG]}{[RG][H]} \quad \beta M = \frac{[RG*]}{[R][G*]} \quad \gamma\beta L = \frac{[HRG*]}{[HRG]}$$

Combining the definitions of the above mentioned reaction constants with the conservation equations for the three components H, R and G yields the following equations for the corresponding free species:

$$[R] = \frac{Rt}{1 + K[H] + M[G](1 + \beta L + \alpha K[H][1 + \beta\gamma L])} \quad \text{eq 1}$$

$$[G] = \frac{Gt}{1 + L + M[R](1 + \beta L + \alpha K[H][1 + \beta\gamma L])} \quad \text{eq 2}$$

$$[H] = \frac{Ht}{1 + K[R] + \alpha KM[G][R](1 + \beta\gamma L)} \quad \text{eq 3}$$

Rt, *Ht*, and *Gt* in eqs 1-3 signify the total concentrations of the corresponding components. Given the reaction constants and total concentrations of the three components, we calculated free concentrations of the three components by solving eqs 1-3 numerically using an algorithm that has been described previously (Costa et al., 1992, Onaran et al., 1993). This algorithm has been proved to converge to a unique solution vector for the free species (Pradines et al., 2001). Once the concentrations of the free species are thus obtained, the concentrations of all the other species can be readily calculated by using the definitions of the reaction constants given above. See the results section for the choice of parameter values.

Other Procedures:

The number of living cells was determined by MTT (Methylthiazolyldiphenyl-tetrazolium bromide) assay as described by the manufacturer (Sigma-Aldrich, Taufkirchen, Germany). Protein concentration in the membrane preparations was determined by Bradford assay using bovine serum albumin as standard (Bradford, 1976).

All standard reagents (buffers, salts, detergents, etc.) were from Sigma-Aldrich, Taufkirchen, Germany or Fisher Scientific, NJ, USA at appropriate purity. βAR ligands were from Tocris Cookson, Bristol, UK. Guanine nucleotides were from Roche Diagnostics, Mannheim, Germany. [125I]-iodocyanopindolol and [125I]-NaI were purchased from Amersham Biosciences, Buckinghamshire, UK. β-adrenoceptor ligands were obtained from the following suppliers: Tocris Cookson (Bristol, UK) for clenbuterol, cimaterol, procaterol hydrochloride, dobutamine hydrochloride, pronethalol hydrochloride, (S)-(-)-propranolol hydrochloride, sotalol hydrochloride, ICI-188,551 hydrochloride, cyanopindolol hemifumarate, (S)-(-)-pindolol, ICI-89,406; Sigma-Aldrich (Taufkirchen, Germany) for (-)-Isoproterenol hydrochloride, (-)-adrenalin, (-)-alprenolol hydrochloride, timolol maleate, terbutaline hemisulphate.

RESULTS

Expression and cellular localization of Gαs and XLαs proteins

Transfection of HEK293 or 2B2 cells with $G\alpha s_L$ or XLαs resulted in considerable overexpression of the proteins in the membrane fractions (figure 2A). Note that HEK293 cells endogenously express the long (52 kDa) and the short (45 kDa) forms of Gαs but not XLαs (94 kDa), whereas the untransfected 2B2 mouse embryonic fibroblasts express neither Gαs nor XLαs due to homozygous ablation of *GNAS* exon 2. Expression levels of $G\alpha s_L$ or XLαs were similar in the 2B2 clones selected for further experiments (see figure 2B). As the similarity of the expression levels has a critical importance for the interpretation of data presented in the following sections, we gave the details of the measurement procedure in supplementary figure 1. cAMP response to agonist stimulation in these clones was restored by $G\alpha s_L$ or XLαs expression (figure 2C).

We used confocal microscopy and transiently transfected HEK293 cells to determine subcellular localization of XLαs or $G\alpha s_L$. Endogenous Gαs in HEK293 cells did not produce a detectable fluorescence signal in untransfected cells, allowing us to distinguish XLαs (or additional $G\alpha s_L$) signal in the transfected HEK293 cells by using an antibody against the common carboxyl terminus of Gαs and XLαs. Localization pattern of the proteins differed considerably among cells for both XLαs and $G\alpha s_L$ (figure 2D): Cell membrane, diffuse cytoplasmic, and perinuclear staining were all evident in both cases. Thus, in HEK293 cells we were unable to diagnose any obvious difference between the distribution patterns of $G\alpha s_L$ and XLαs as opposed to what has been reported previously (Kehlenbach et al., 1994; Uğur and Jones 2000; Linglart et al. 2006). Despite the diffuse cytoplasmic staining in some cells we found no XLαs in soluble fractions of the cell homogenates, which indicated that XLαs

JPET Fast Forward. Published on January 14, 2009 as DOI: 10.1124/jpet.108.149989
This article has not been copyedited and formatted. The final version may differ from this version.

was mostly associated with membranes. Unlike XLαs, a small fraction of Gαs could be found in the soluble fractions (data not shown).

Despite the obvious expression of $G\alpha s_L$ or XLαs (figure 2A-C) in stably transfected 2B2 clones we failed to obtain a good quality immunostaining for $G\alpha s_L$ or XLαs in these cells due to a high background signal that resulted apparently from the nonspecific interactions of the fluorescent antibodies with some constituents of the 2B2 cells.

Stimulation of adenylyl cyclase activity

We measured cAMP production in the presence or absence of βAR ligands in intact HEK293 cells co-transfected with βAR and XLαs or $G\alpha s_L$. As shown in figure 3A, cells transfected with XLαs showed higher basal and agonist stimulated cAMP accumulation than those transfected with Gαs, although the expression levels of each G protein α-subunit and the βAR were comparable. In $G\alpha s_L$ transfected cells, inverse agonists timolol and ICI118,551 reduced the basal cAMP levels. On the other hand, the basal cAMP level in XLαs transfected cells was not responsive to these inverse agonists (figure 3A). Thus, we asked whether the elevated basal XLαs activity was independent of receptor coupling. Increasing the level of βAR expression resulted in an increase of basal cAMP accumulation in both $G\alpha s_L$- and XLαs-transfected cells, demonstrating that the high basal activity of XLαs is associated, at least partly, with the receptor. At the high receptor expression levels, the basal cAMP level in XLαs-transfected cells remained insensitive to inverse agonists (figure 3A, right panel).

One interpretation for this result might be that XLαs was partially or completely unable to distinguish between the inverse agonist-bound and the empty receptor conformations. However, a more comprehensive scenario can also explain this observation, along with the observations presented below, by a different mechanism (see discussion).

JPET Fast Forward. Published on January 14, 2009 as DOI: 10.1124/jpet.108.149989
This article has not been copyedited and formatted. The final version may differ from this version.

In order to observe pure XLαs response to βAR and to avoid possible interference of endogenous Gαs, we used the Gαs-deficient 2B2 cells. As expected, cAMP production of these cells was insensitive to β-adrenergic stimulation. Transfection of these cells with XLαs or $G\alpha s_L$ restored the cAMP response, as a small amount of βAR (~100 fmol/mg) is expressed endogenously (figure 2C). We nevertheless stably overexpressed βAR along with XLαs or Gαs for examining basal receptor activity, which was otherwise undetectable. Selected clonal cells expressed comparable levels of $G\alpha s_L$ and XLαs (figure 2B). At ~1 pmol/mg of βAR, the basal cAMP level in XLαs-transfected cells was unaltered in response to inverse agonists (figure 3B, left panel). When the receptor expression level was increased to ~5 pmol/mg, an inverse agonist effect of ICI118,551 emerged in XLαs transfected cells as well (figure 3B, right panel), but the magnitude of this effect was small compared to that observed in $G\alpha s_L$-transfected cells; ICI118,551-induced inhibition of basal activity was 65% in $G\alpha s_L$, but was 30% in XLαs-transfected cells. These results confirmed the above observation that XLαs-transfected cells were more resistant to inverse agonist effects than Gαs-transfected cells.

The observation that inverse agonist-induced responses of $G\alpha s_L$ and XLαs were different from one another suggested that variation in receptor state which can be induced by different ligands, is also perceived differently by these two proteins. We thus systematically screened a set of βAR ligands with a broad spectrum of efficacy for their ability to stimulate cAMP accumulation in $G\alpha s_L$- or XLαs-transfected cells. Figure 4A-B shows cAMP responses of $G\alpha s_L$- or XLαs-transfected 2B2 cells that overexpress βAR at a level of ~1 or ~5 pmol/mg. Overall, relative intrinsic activity of each ligand observed in XLαs-transfected cells was comparable to that in $G\alpha s_L$-expressing cells. While the basal cAMP accumulation was relatively high in XLαs-transfected cells (consistent with results presented above), the difference between XLαs and $G\alpha s_L$ was less evident upon agonist stimulation. At ~1

JPET Fast Forward. Published on January 14, 2009 as DOI: 10.1124/jpet.108.149989
This article has not been copyedited and formatted. The final version may differ from this version.

pmol/mg receptor expression, maximal cAMP accumulation was similar in XLαs- and $G\alpha s_L$-transfected cells for strong, but not for partial, agonists (figure 4A). When the receptor expression was increased to ~5 pmol/mg, the similarity between XLαs and Gαs transfected cells in terms of maximal cAMP accumulation was also observed for the partial agonist dobutamine (figure 4B). We were unable to further increase the receptor expression in 2B2 cells. Thus, to address the question as to whether higher receptor expression levels would result in similar levels of XLαs- and Gαs- mediated maximal cAMP accumulation even in response to agonists with lower efficacy than dobutamine, we used HEK293 cell clones that express βAR at a level of 30 pmol/mg. At this receptor expression level the difference between XLαs- and $G\alpha s_L$-mediated cAMP accumulation responses to agonists was no longer detectable: Even those agents with very low intrinsic activity, starting from propranolol which displayed a weak agonistic effect at this level of receptor expression, were able to stimulate XLαs and $G\alpha s_L$ equally well (Figure 4C). This phenomenon is best seen when the responses are shown on normalized scales (Figure 4D). In figure 4D three categories of ligands are identifiable: 1) ICI118,551, timolol, sotalol, for which XLαs is more efficient than $G\alpha s_L$ in mediating cAMP production, 2) from propranolol to pindolol, for which XLαs and $G\alpha s_L$ are equally efficient, and 3) from partial agonist dobutamine to full agonist clenbuterol, for which overexpression of XLαs or Gαs did not increase the response any more than that obtained in HEK293 cells that overexpress βAR only. Together, these results suggested that XLαs is intrinsically more efficient than $G\alpha s_L$ in mediating receptor-induced cAMP accumulation, but this phenomenon is observed when the ligand's efficacy and/or the receptor expression level are relatively low.

A more detailed analysis of the response pattern of weak and inverse agonists is given in figure 4E for intermediate level of receptor expression, where the discrepancy between $G\alpha s_L$

JPET Fast Forward. Published on January 14, 2009 as DOI: 10.1124/jpet.108.149989
This article has not been copyedited and formatted. The final version may differ from this version.

and XLαs was best seen. In figure 4E, maximal cAMP accumulations in the presence of indicated ligands in $G\alpha s_L$-transfected 2B2 cells are plotted against those that were obtained in XLαs-transfected cells, where it is evident that XLαs mediates (partial) agonist responses better than $G\alpha s_L$ but is relatively insensitive to inverse agonist-induced inhibition of basal activity as assessed by the slopes of the lines in figure 4E.

Ligand Binding

The above observation that XLαs mediates βAR signaling more efficiently than $G\alpha s_L$ (at least conditionally) suggests that XLαs couples better to βAR and/or stimulates adenylyl cyclase more efficiently than does $G\alpha s_L$. Although the findings presented above (figure 4) are consistent with the former possibility, more direct evidence for this possibility could be obtained by using a ligand binding strategy; the efficiency of receptor-G protein coupling should affect agonist binding pattern, whereas that of G protein-effector coupling is not expected to have a consequence on ligand binding. Therefore, we analyzed agonist binding affinity of βAR in 2B2 cells expressing XLαs or $G\alpha s_L$ in the presence or absence of guanine nucleotides. This setting can be considered as an experimental paradigm in the framework of ternary complex-like models to reveal the efficiency of receptor-G protein coupling. As shown in figure 5 and table 1, in the presence of GDP+AlF, isoproterenol bound to βAR with low affinity both in XLαs and $G\alpha s_L$ expressing cell membranes. In the absence of the guanine nucleotide, the binding isotherm fit to a double-site binding model in both cases. In fact, the low affinity values estimated from the double-site fit in the absence of the guanine nucleotide were consistent with those estimated in the presence of the guanine nucleotide. Increasing the receptor expression reduced the proportion of high affinity binding sites and nucleotide-induced shift without affecting the binding affinities (table 1), which is consistent with the predictions of the ternary complex model. The proportion of high affinity binding sites was

JPET Fast Forward. Published on January 14, 2009 as DOI: 10.1124/jpet.108.149989
This article has not been copyedited and formatted. The final version may differ from this version.

higher in XLαs expressing cells than in $G\alpha s_L$ expressing cells, and the nucleotide-induced shifts in isoproterenol binding were more pronounced in membrane preparations from XLαs expressing cells. Finally, binding affinity for high-affinity binding sites was higher in XLαs expressing than in $G\alpha s_L$ expressing cells. We obtained similar results in HEK293 cells that overexpress βAR and XLαs or $G\alpha s_L$ (see supplementary figure 2). Combined, these results show that βAR-G protein coupling is more efficient in the case of XLαs than $G\alpha s_L$.

Numerical Simulations

Numerical simulations that are made by using the scheme in figure 1 are shown in Figure 6. Gαs and XLαs are simulated as possessing different affinities for the receptor ($M=5x10^9$ M^{-1} for Gαs, and $M=3x10^{11}$ M^{-1} for XLαs). Ligands were simulated as follows: Inverse agonist ($\alpha<1$, $\gamma=1$), neutral ligand ($\alpha=1$, $\gamma=1$), agonist ($\alpha>1$, $\gamma>1$). In the case of agonism, values of α and γ were chosen equal for simplicity and changed together to simulate partial and full agonists. The value of γ for inverse agonists was set to 1 (see below). For a particular ligand type, values of α and γ were set constant when simulating different types of G proteins. Following parameters were constant for different G protein and ligand types: $\beta=20$, $K=10^7$ M^{-1}, $[G_{total}]=10^{-10}$ M, and $L=[G^*]/[G]=0.01$ yielding a very low spontaneous G protein activity in the absence of receptor intervention. The first row of figure 6A shows the predicted G protein activation depending on receptor density in the absence or saturating presence of three kinds of ligands; an inverse agonist, a partial or a full agonist. Note that the activation induced by the partial agonist differs for the two G proteins only at low receptor concentrations ($[R_t] \cong 10^{-10}$ M). This difference disappears at high receptor concentrations ($[R_t] \cong 10^{-9}$ M), and the activation of the two G proteins by the partial agonist becomes equal at a level below the maximal response of the system (compare the saturation levels obtained in the case of partial and full agonist in the first row of figure 6A). This prediction is

consistent with the experimental observations presented in figure 4A-C. The second row of figure 6A shows the formation of RG complex, which can be considered as what the traditional interpretation of the ternary complex would predict for activation in corresponding situations. In the latter case, as opposed to the former, the system is predicted to be maximally active when the difference between the two G proteins disappears (compare the saturation levels obtained in the case of partial and full agonist in the second row of figure 6A), which was not the case experimentally. The assumption that inverse agonists, as opposed to agonists, do not affect G protein activation directly (γ=1) leads to the discontinuity observed in the experiments (compare figures 6B and 4E). Interestingly, the present model also predicts that the inverse agonist effect should have a maximum (more pronounced for Gαs than XLαs) depending on receptor expression, and this was observed experimentally (see figures 6C and 6D). Although not demonstrated numerically in the present report the entire scenario is compatible with the binding patterns observed in figure 5.

DISCUSSION

We investigated receptor coupling properties of Gαs and its variant XLαs, revealing that XLαs couples βAR signaling to adenylyl cyclase more efficiently than $G\alpha s_L$. The difference between XLαs and $G\alpha s_L$ was apparently due to the difference between coupling abilities of these G proteins to the receptor.

Gαs is required for numerous agonist responses. Unlike Gαs, which is ubiquitous, XLαs seems to be more abundant in neuroendocrine tissues and brain (Kehlenbach et al., 1994; Passolli et al., 2000), although XLαs transcript has been detected in many different tissues (Hayward et al., 1998; Plagge et al., 2004). The phenotypes observed from mice in which either XLαs or Gαs is knocked out alone suggest that these two proteins have markedly different physiological roles (Plagge et al., 2004; Chen et al., 2005; Germain-Lee et al., 2005). While the unique cellular roles of XLαs remain to be defined, it has been clearly shown that XLαs can mediate cyclase stimulation in response to receptor activation (Klemke et al., 2000; Bastepe et al., 2002; Linglart et al., 2006). Our results now verify these findings and suggest furthermore that XLαs may be an important contributor of cAMP signaling, even in tissues where XLαs levels are markedly lower than Gαs levels. Consistent with this prediction, XLαs mRNA is markedly lower than Gαs mRNA in growth plate chondrocytes, but XLαs ablation together with the ablation of one Gαs copy (paternal Gnas exon 2 disruption) results in a more severe phenotype, i.e. premature chondrocyte hypertrophy, than the ablation of one Gαs copy alone (maternal Gnas exon 2 disruption) (Bastepe et al., 2004). cAMP signaling is involved in a vast majority of cellular responses, and the superiority of XLαs over Gαs in terms of receptor coupling and cAMP generation may thus have important implications in physiology and diseases. Naturally occurring *GNAS* mutations, with the exception of those located in exon 1, are predicted to affect not only Gαs but also XLαs. The changes in XLαs activity can

JPET Fast Forward. Published on January 14, 2009 as DOI: 10.1124/jpet.108.149989
This article has not been copyedited and formatted. The final version may differ from this version.

be involved in the pathogenesis of diseases caused by these mutations, such as various endocrine and non-endocrine tumors (activating) or Albright's hereditary osteodystrophy (inactivating).

In a series of studies, divergent signaling abilities of $G\alpha s_L$ and $G\alpha s_S$ (splice variants of $G\alpha s$) have been reported, where the difference was attributed to a higher rate of dissociation of GDP from $G\alpha s_L$ than $G\alpha s_S$ (Seifert et al., 1998; Wenzel-Seifert et al., 2001, 2002). In these studies, receptor-G protein fusions were used in order to obtain 1:1 stochiometry of receptor:G protein, which provided a good model for investigating the coupling efficiency between receptor and G protein. In the present work, however, βAR-XLαs fusion protein did not function in 2B2 cells, while mediating agonist-induced cyclase activation in HEK293 cells (see supplementary figure 3 and 4). Interactions of receptor or G protein in the fusion protein with their non-fused partners in the cell membrane have been reported (Burt et al., 1998; Molinari et al., 2003). Hence, the observed discrepancy between HEK293 and 2B2 cells that express βAR-XLαs fusion protein can be interpreted as follows: The receptor in the fusion construct interacts fruitfully with endogenously expressed Gαs proteins, which is present in HEK293 but not in 2B2 cells. Hence, no response is observed in 2B2 cells as no intra- or inter-fusion interaction can actually occur between receptor and XLαs (see supplementary figure 3 for a schematic representation of the idea). Therefore, we were unable to compare XLαs and $G\alpha s_L$ in the fusion model. Thus, receptor:G protein stochiometry was variable (but controlled) in our experiments; this variability, on the other hand, eventually proved to be an advantage for the present case (see below).

Strikingly, the observed difference between XLαs- and $G\alpha s_L$ was conditional. It disappeared with increasing ligand efficacy, threshold of which was dependent on the expression level of the receptor (figure 4). At first sight, this observation implies a saturation effect in the

JPET Fast Forward. Published on January 14, 2009 as DOI: 10.1124/jpet.108.149989
This article has not been copyedited and formatted. The final version may differ from this version.

receptor-G protein coupling. However, cyclase activities mediated by XLαs or $G\alpha s_L$ became comparable at a level far below the full agonist-induced maximal cyclase activity observable in the cells (figure 4 B and C). Hence, this pattern requires further considerations in the framework of the interpretation of ternary complex models that have been used successfully to explain ligand behavior. What is not compatible with this framework is the following: In a system where a receptor couples with different efficiencies to two different G proteins, which in turn, transmit the receptor signal to a unique effector with the same efficiency, the models predict that the ligand-induced effector activations that are mediated by these two G proteins cannot be equal when the stimulated response is below the maximal response of the system. Hence, the models, in their currently interpreted forms, cannot predict the observed equalization of Gαs- and XLαs-mediated responses below the maximum level of adenylyl cyclase activation that is achievable in the presence of full βAR agonists. This "defect", which is not an intrinsic property of the ternary complex models, stems from the assumption that receptor-bound G protein is fully active, and can easily be eliminated by assuming that formation of receptor-G protein complex is not necessarily equivalent to full activation of G protein, and that agonist binding to receptor can have further "activating" effects on the G protein via conformational changes when receptor and G proteins are bound to each other. Such a scenario has already been suggested for rhodopsin-Gt interaction (Fanelli and Dell'Orco, 2005). Consequences of this assumption become obvious when we introduce G protein activation into the ternary complex model as a simple two-state process (G-active or G-inactive; shown in figure 1). Inclusion of a G protein activation step in the ternary interaction scheme inevitably divides the ligand efficacy into two parts: Ability of ligand to modify R-G binding (governed by the allosteric constant α in figure 1), and to modify G protein activation (i.e. G-G* transition) in the RG complex (governed by the allosteric constant γ in figure 1). On the basis of these fundamentals the observed behavior of XLαs and

JPET Fast Forward. Published on January 14, 2009 as DOI: 10.1124/jpet.108.149989
This article has not been copyedited and formatted. The final version may differ from this version.

Gαs in mediating βAR signal can be explained almost entirely by making the following additional assumptions (see figure 6): XLαs and $G\alpha s_L$ differ only in their unconditional tendency to bind receptor ($M_{XL\alpha s} > M_{G\alpha sL}$); efficacy of ligands on βAR does not depend on the identity of G protein to which the receptor is coupled (at least in the case of XLαs and $G\alpha s_L$); spontaneous tendency of RG complex to get activated is relatively low ($L<<1$ and $1<\beta$); efficacy of neutral or agonist ligands are evenly distributed over α and γ (for the sake of simplicity); and finally, inverse agonists have no direct effect on G protein activation (i.e. $\gamma=1$) but reduces RG binding (i.e. $\alpha<1$). The last assumption is rather speculative, but required to explain the inverse agonist effect on βAR-XLαs coupling compared to $G\alpha s_L$. In this framework, the basic mechanism and the scenario that explains the advantage of XLαs over $G\alpha s_L$ depending on ligand efficacy and receptor expression can be stated as follows: The origin of difference between the two G proteins is their diverging affinities for the receptor, which is operative (and observable) only when RG interaction is not saturated. The saturation depends on the combined effect of receptor expression and ligand efficacy. Once RG saturation occurs, the difference between XLαs and $G\alpha s_L$ disappears, since ligands are assumed to have γ values that do not depend on the kind of G protein. However, even at this saturation point weak agonists do not necessarily induce maximal response of the system (i.e. G-G* conversion in RG complex may not be complete upon agonist binding depending on the γ value of the agonist) (see figure 6). This scenario also supports a long debated idea that inactive receptor and G protein tend to form an RG complex that does not necessarily lead to G protein activation, which actually occurs upon activation of receptor in the complex. Accordingly, agonist-induced (or spontaneous) receptor activation directly transmits an activating conformational signal to a precoupled G protein without necessarily affecting the stability of the RG complex. Several lines of indirect evidence support this statement (see for example Fanelli and Dell'Orco, 2005).

In summary, the present study showed that βAR can couple to XLαs better than Gαs, and that the rank order of ligand efficacies does not change when it is coupled to XLαs. Thus, despite the differences observed between Gαs and XLαs signaling, no ligand-dependent divergence is predicted to occur between XLαs and Gαs in transmitting βAR signal to adenylyl cyclase. Nevertheless, βAR signaling becomes relatively resistant to inverse agonists when the receptor is coupled to XLαs, which may have pharmacological implications depending on the distribution of βAR-XLαs coupling in the body. This may justify further studies on βAR-XLαs coupling (or receptor-XLαs coupling in general) in physiological integrity. Finally, the experimental system where the two kinds of G proteins are coupled to the same receptor with different efficiencies enabled us to re-evaluate the interpretation of the ternary complex model, especially when it is used to explain or understand G protein activation.

REFERENCES

Bastepe M, Güneş Y, Perez-Villamil B, Hunzelman J, Weinstein LS and Jüppner H (2002) Receptor mediated adenylyl cyclase activation through XLαs, the extra large variant of the stimulatory G protein α-subunit. *Mol Endocrinol* **16:** 1912-1919.

Bastepe M, Weinstein LS, Ogata N, Kawaguchi H, Jüppner H, Kronenberg HM and Chung U (2004) *Proc Natl Acad Sci* USA **101**: 14794-14799.

Bradford MM (1976) A rapid and sensitive method for the quantitation of microgram quantities of protein utilizing the principle of protein-dye binding. *Anal Biochem* **72:** 248-254.

Bray P, Carter A, Simons C, Guo V, Puckett C, Kamholtz J, Spiegel A and Nirenberg M (1986) Human clones for four species of Gsα signal transduction protein. *Proc Natl Acad Sci USA* **83:** 8893–9997.

Burt AR, Sautel M, Wilson MA, Rees S, Wise A and Milligan G (1998) Agonist occupation of an α_{2a}-adrenoreceptor-$G_{i1}\alpha$ fusion protein results in activation of both receptor-linked and endogenous Gi proteins: Comparisons of their contributions to GTPase activity and signal transduction and analysis of receptor-G protein activation stoichiometry. *J Biol Chem* **273:** 10367–10375.

Chen M, Gavrilova O, Liu J, Xie T, Deng C, Nguyen AT, Nackers LM, Lorenzo J, Shen L and Weinstein LS (2005) Alternative Gnas gene products have opposite effects on glucose and lipid metabolism. *Proc Natl Acad Sci* USA **102**:7386-7391.

Costa T, Ogino Y, Munson PJ, Onaran HO, Rodbard D (1992) Drug efficacy at guanine nucleotide-binding regulatory protein-linked receptors: Thermodynamic interpretation of negative antagonism and of receptor activity in the absence of ligand. *Mol Pharmacol* **41**: 549-560.

Fanelli F, Menziani C, Scheer A, Cotecchia S, De Benedetti PG (1999) Theoretical study of the electrostatically driven step of receptor-G protein recognition. *Proteins* **37:** 145-156.

Fanelli F and Dell'Orco D (2005) Rhodopsin activation follows precoupling with transducin: Inferences from computational analysis. *Biochemistry* **44:** 14695-14700.

Freson K, Hoylaerts MF, Jaeken J, Eyssen M, Arnout J, Vermylen J, Van Geet C (2001) Genetic variation of the extra-large stimulatory G protein alpha-subunit leads to Gs hyperfunction in platelets and is a risk factor for bleeding. *Thromb Haemost* **86:** 733-738.

Germain-Lee EL, Schwindinger W, Crane JL, Zewdu R, Zweifel LS, Wand G, Huso DL, Saji M, Ringel MD and Levine MA (2005) A mouse model of Albright Hereditary osteodistrophy generated by targeted disruption of exon 1 of the Gnas gene. *Endocrinology* **146**: 4697-4709.

Geneviève D, Sanlaville D, Faivre L, Kottler ML, Jambou M, Gosset P, Boustani-Samara D, Pinto G, Ozilou C, Abeguilé G, Munnich A, Romana S, Raoul O, Cormier-Daire V, Vekemans M (2005) Paternal deletion of the GNAS imprinted locus (including Gnasxl) in two girls presenting with severe pre- and post-natal growth retardation and intractable feeding difficulties. *Eur J Hum Genet* **13:** 1033-1039.

Gilman AG (1987) G proteins: transducers of receptor-generated signals. *Ann Rev Biochem* **56:** 615–649.

Gulick T (1997) Transfection using DEAE-Dextran. *Current Protocols in Molecular Biology*. John Wiley & Sons, Inc, pp 9.2.1-9.2.10.

Hamm HE (1998) The many faces of G protein signaling. *J Biol Chem* **273:** 669-672.

Hayward BE, Kamiya M, Strain L, Moran V, Campbell R, Hayashizaki Y and Bonthron DT (1998) The human *GNAS* 1 gene is imprinted and encodes distinct paternally and biallelically expressed G proteins. *Proc Natl Acad Sci* USA **95**:10038-10043.

Kehlenbach RH, Mattley J and Huttner WB (1994) XLαs is a new type of G protein. *Nature* **372:** 804-809.

Kehlenbach RH, Matthey J, Huttner WB (1995) XLαs is a new type of G protein. *Nature* **375:** 253.

Kingston RE, Chen CA, Okayama H and Rose JK (1996) Transfection of DNA into eukaryotic cells. *Current Protocols in Molecular Biology*. John Wiley & Sons, Inc., pp 9.1.1-9.1.11.

Klemke M, Pasolli HA, Kehlenbach RH, Offermannsi S, Schultzi G and Huttner WB (2000) Characterization of the extra-large G protein α-subunit XLαs. II. Signal transduction properties. *J Biol Chem* **275:** 33633-33640.

Kozasa T, Itoh H, Tsukamoto T and Kaziro Y (1988) Isolation and characterization of the human Gsα gene. *Proc Natl Acad Sci USA* **85:** 2081–2085.

Linglart A, Maohn MJ, Kerachian MA, Berlach DM, Hendy GN, Jüppner H and Bastepe M (2006) Coding *GNAS* mutations leading to hormone resistance impair *in vitro* agonist- and cholera toxin-induced adenosine cyclic 3',5'-monophosphate formation mediated by human XLαs. *Endocrinology* **147:** 2253-2262.

Molinari P, Ambrosio C, Riitano D, Sbraccia M, Gró MC and Costa T (2003) Promiscuous Coupling at Receptor-Gα Fusion Proteins: The receptor of one covalent complex interacts with the α-subunit of another. *J Biol Chem* **278:** 15778–15788.

Onaran HO, Costa T, Rodbard D (1993) βγ-Subunits of guanine nucleotide-binding proteins and regulation of spontaneous receptor activity: thermodynamic model for the interaction between receptors and guanine nucleotide-binding protein subunits. *Mol Pharmacol* **43**: 245-256.

Pasolli HA, Klemke M, Kehlenbach RH, Wang Y, and Hutter WB (2000) Characterization of the extra-large G protein α-subunit XLαs. I. Tissue distribution and subcellular localization. *J Biol Chem* **275:** 33622-33632.

Plagge A, Gordon E, Dean W, Boiani R, Cinti S, Peters J and Kelsey G (2004) The imprinted signaling protein XLαs is required for postnatal adaptation to feeding. *Nat Genetics* **36:** 818-826.

Pradines JR, Hasty J, Pakdaman K (2001) Complex ligand-protein systems: a globally convergent iterative method for the n×m case. *J Math Biol* **43**: 313-324.

Seifert R, Wenzel-Seifert K, Lee TW, Gether U, Sanders-Bush E, and Kobilka BK (1998) Different effects of Gsα splice variants on β2-adrenoreceptor-mediated signaling. The β2-adrenoreceptor coupled to the long splice variant of Gsα has properties of a constitutively active receptor. *J Biol Chem* **273:** 5109–5116.

Uğur Ö, and Onaran HO (1997) Allosteric equilibrium model explains steady-state coupling of beta-adrenergic receptors to adenylate cyclase in turkey erythrocyte membranes. *Biochem J* **323:** 765-776.

Uğur O and Jones TLZ (2000) A proline-rich region and nearby cysteine residues target XLαs to the golgi complex region. *Mol Biol Cell* **11:** 1421-1432.

Wenzel-Seifert K, Kelley MT, Buschauer A and Seifert R (2001) Similar apparent constitutive activity of human histamine h2-receptor fused to long and short splice variants of Gsα. *J Pharmacol Exp Ther* **299:** 1013-1020.

Wenzel-Seifert K, Liu HY and Seifert R (2002) Similarities and differences in the coupling of human β_1- and β_2-ARs to $G_{s\alpha}$ splice variants. *Biochem Pharmacol* **64:** 9-20.

FOOTNOTES

This work was supported, in part, by research grants from Turkish Scientific and Technical Research Council [104s472], Ankara University Research Fund [BAP 2002 0809 088], Ankara University Biotechnology institute [103], and The National Institute of Diabetes and Digestive and Kidney Diseases to MB [R01DK073911] (the content is solely the responsibility of the authors and does not necessarily represent the official view of the National Institute of Diabetes and Digestive and Kidney Diseases or the National Institutes of Health).

Send reprint requests to: H. Ongun Onaran, Ankara Üniversitei Tıp Fakültesi, Farmakoloji ve Klinik Farmakoloji Ab.D. Sıhhiye 06100 Ankara, Turkey. Phone: +90 312 311 8829, Fax: +90 312 310 6268, e-mail: onaran@medicine.ankara.edu.tr

1. Present address: Dept. Cell and Molecular Pharmacology, Medical University of South Carolina, Charleston, SC, USA.

JPET Fast Forward. Published on January 14, 2009 as DOI: 10.1124/jpet.108.149989
This article has not been copyedited and formatted. The final version may differ from this version.

LEGENDS FOR FIGURES

Figure 1

Description of the equilibrium model where the ternary complex model was extended to include G protein activation (G-G* transition) explicitly. Left panel: meanings of the parameters are given schematically: Three binding partners are designated as H, R, G for ligand, receptor and G proteins respectively. Binding sites on the proteins are shown as black circles. Activation of G protein is symbolized as a grey area in the G protein, in which the activation reaction (*↔0) takes place. Three reaction constants (K, M, and L) for relevant binding (or isomerization) reactions, and three allosteric couplings (α, β, and γ) that links these reactions are indicated on the picture. Among the allosteric factors, γ is a second order effect that is transmitted between ligand binding and G protein activation reactions once the RG complex is formed. Note that ligand efficacy in the model comprises of the mixed effects of α and γ. Right panel: Equilibrium reactions and corresponding equilibrium constants are shown. Elementary reactions are indicated with thick lines.

Figure 2

Expression of $G\alpha s_L$ or XLαs in HEK293 or 2B2 cells. (**A**) Representative Western blots of membrane preparations from transiently transfected HEK293 or permanently cloned 2B2 cells as indicated in the picture; ϕ, G and X signify no transfection, transfection with $G\alpha s_L$ or XLαs respectively. (**B**) Densitometric analysis of 2B2 cell clones which were used throughout the present experiments. Mean values (bars) were calculated from four independent membrane preparations (for each clone) by using three serial dilutions (5, 2.5, 1.25 μg/ per lane) for each preparation. Lines on the bars represent S.E.M. No significant difference were found between $G\alpha s_L$ and XLαs signals in these clones ($p>0.05$, as assessed by Student's t test). (**C**)

Intracellular cAMP accumulation in untransfected cells, or in Gαs_L or XLαs expressing 2B2 cell clones measured in the presence of 0.1 mM isoproterenol. cAMP response were normalized to the number of living cells in the wells as assed by parallel MTT assays. The numerical value of the MTT signal was ~0.3 on average. Response in transfected cells is presented as average response as we observed no significant difference between Gαs_L or XLαs expressing clones. (**D**) Cellular distribution of Gαs_L or XLαs in HEK293 cells that overexpress βAR. Cells were transfected with the cDNA of Gαs_L or XLαs (as indicated in the picture) and confocal images were obtained after immunostaining by using an antibody against the carboxyl terminus of Gαs (the same antibody was used in the immunoblotting experiments). Each picture consist of a collage of cell images chosen intentionally to show that the distribution pattern of both Gαs_L and XLαs exhibits a cell-to-cell variation. Scaling bars on the pictures are 10 μm.

Figure 3

Cyclic AMP responses in HEK293 (**A**) or 2B2 (**B**) cells in the absence or presence of saturating concentrations of indicated ligands. The level of βAR expression in each cell type is indicated in the picture. Gαs_L and XLαs expression levels were comparable in these cells as explained in figure 2B. cAMP response were normalized to the number of living cells in the wells as assed by parallel MTT assays. The numerical value of the MTT signal was ~0.3 on average. Results are mean (+ S.E.M.) values of 10 (**A**) or 8 (**B**) independent quadruplicate experiments.

Figure 4

Cyclic AMP responses in the absence or presence of saturating concentrations of indicated ligands in the cells that express comparable amount of Gαs_L or XLαs, but varying level of

JPET Fast Forward. Published on January 14, 2009 as DOI: 10.1124/jpet.108.149989
This article has not been copyedited and formatted. The final version may differ from this version.

βAR: (**A**) 2B2 cells expressing 1 pmol/mg of βAR, (**B**) 2B2 cells expressing 5 pmol/mg of βAR, (**C**) HEK293 cells expressing 30 pmol/mg of βAR. Ligand concentrations were 10^{-6} or 10^{-4} M depending on ligand's affinity to βAR. Results are mean (+ S.E.M.) values of 3 to 4 independent quadruplicate experiment. cAMP response were normalized to the number of living cells in the wells as assed by parallel MTT assays. Significant differences in panels **A-C** are shown with the symbol (*), as assessed by Student's test. Two cases were considered as noise: marginal difference (p=0.06) in sotalol in panel C, and significant difference in clenbuterol in panel A (p<0.05). (**D**) Increase in cAMP response upon transfection of HEK293 cells (that express 30 pmol/mg of βAR) with $G\alpha s_L$ or XLαs was given as fold increase in cAMP response relative to vector transfected cells that express the same amount of βAR in the absence or presence of indicated ligands. The plot is constructed by dividing the data given in panel **C** by the response observed in vector transfected cells. Three groups of ligands are indicated in the picture (see text). (**E**) cAMP responses in 2B2 cells that express $G\alpha s_L$ were plotted against cAMP responses in 2B2 cells that express XLαs in the absence or presence of following ligands that include inverse agonists and very weak partial agonists: 1:ICI118,551, 2:Timolol, 3:Sotalol, 4:Propranolol, 5:ICI 89,406, 6:no ligand, 7:Pronethalol, 8:Cyanopindolol, 9:Pindolol, 10:Alprenolol (data are from panel **B**). Data are fitted with two straight lines having different slopes. Slopes of the lines differ by a factor of 3.

Figure 5

Competition binding curves ([125I]-Iodocyanopindolol vs. isoproterenol) obtained in the membranes from 2B2 cell clones that express comparable amount of $G\alpha s_L$ or XLαs and indicated amounts of βAR. Binding curves were obtained in the absence or presence of GDP (10 μM) +$AlCl_3$ (20 μM) + NaF (10 mM) as indicated in the picture. Binding of hot ligand is given as a fraction of total receptor (Rt) in each case. Solid curves are nonlinear regressions of

numerically solved competition-binding equations for two binding sites. Areas between binding curves obtained in the absence or presence of nucleotide (ΔAUC) are given in the pictures as a measure of nucleotide-induced shift in binding. See table 1 for estimated parameters. Data are mean (± S.E.M.) values of three independent quadruplicate experiments.

Figure 6

Numerical simulations by using the model given in figure 1. (**A**) G protein activation (i.e. G* formation) in the presence or absence of saturating concentrations of indicated type of ligands is given in the first row as a fraction of total G (i.e. [G*+RG*+HRG*]/[total G]) depending on receptor concentration. Fractional formation of RG complex in corresponding situations is given in the second row as indicated in the picture (see text for parameter values). (**B**) G protein activity in the presence (or absence) of inverse agonists and weak partial agonists were simulated for XLαs or Gαs according to the model described in figure 1 at a constant receptor concentration ($R_{total}=2x10^{-10}$ M). Activity (i.e. total G*/total G) calculated for Gαs was plotted against the one that was calculated for XLαs in the presence of different ligands (represented by each dot in the picture). XLαs and Gαs were simulated as in panel A (i.e. with different M values for R). Ligands were simulated as follows: Inverse agonists (α=0.125, 0.25, 0.5; γ=1), neutral antagonist (α=1;γ=1); partial agonists (α = γ = 1.15, 1.32, 1.52, 1.75, 2.01, 2.31). Values of all other parameters are the same as in panel A. The position of neutral ligand is indicated with two dotted lines in the picture. Simulated results were in good agreement with the experimental data given in figure 4E. (**C**) Relative response of an inverse agonist (i.e. activity in the presence of ligand/basal activity) was simulated for XLαs or Gαs at varying receptor concentrations as indicated in the picture. XLαs and Gαs were simulated as in panel A and B. Inverse agonist was simulated with the parameters α=0.1;γ=1. (**D**) Experimentally observed relative response to inverse agonist ICI118,551 (i.e. cyclase activity

in the presence of ICI118,551/basal cyclase activity) at three different receptor concentrations in XLαs or $G\alpha s_L$ expressing cells as indicated in the picture. Data in the picture were calculated from the data given figure 4A-C for ICI118,551. The simulation in panel C is in good agreement with the experimental data.

JPET Fast Forward. Published on January 14, 2009 as DOI: 10.1124/jpet.108.149989
This article has not been copyedited and formatted. The final version may differ from this version.

Table 1. Estimated parameters of isoproterenol binding curves in 2B2 cells that express βAR receptors at two different levels, and XLαs or $G\alpha s_L$ at similar levels.

		Low βAR		High βAR	
		$G\alpha s_L$	XLαs	$G\alpha s_L$	XLαs
	$\log(K_L)$	6.3 ± 0.06	6.5 ± 0.06	6.3 ± 0.05	6.4 ± 0.03
	$\log(K_H)$	8.1 ± 0.12	8.9 ± 0.05	8.2 ± 0.05	8.7 ± 0.05
GDP+AlF	R_L (%)	97 ± 0.2	91 ± 3	95 ± 1	90 ± 4
	R_H (%)	3 ± 0.2	9 ± 3	5 ± 1	10 ± 4
No nucleotide	R_L (%)	59 ± 5	49 ± 5	78 ± 3	59 ± 3
	R_H (%)	41 ± 5	51 ± 5	22 ± 3	41 ± 3
	βAR pmol/mg	0.4 ± 0.02	1.0 ± 0.04	4.9 ± 0.53	3.5 ± 0.22

Parameters are estimated by the regression of numerical solution of competition binding equations assuming a single dissociation constant of 40 pM for [125I]-iodocyanopindolol. Affinities for isoproterenol were estimated simultaneously by sharing the parameters between two curves obtained in the presence or absence of GDP;AlF (100 μM;10 mM). This procedure did not cause a significant worsening of residual variance compared to independent estimation of the parameters ($p > 0.05$ as assessed by F statistics). Percent contributions of high and low affinity components are indicated as R_H and R_L and corresponding affinities as K_H and K_L (see figure 5 for the biding curves).

Figure 1

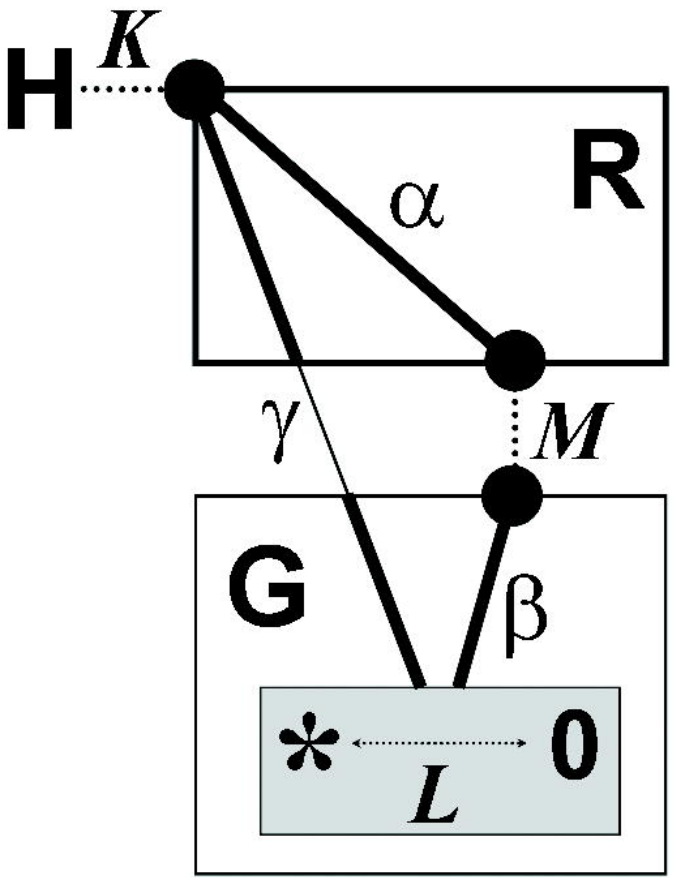
H
K
R
α
γ
M
G
β
*
L
0

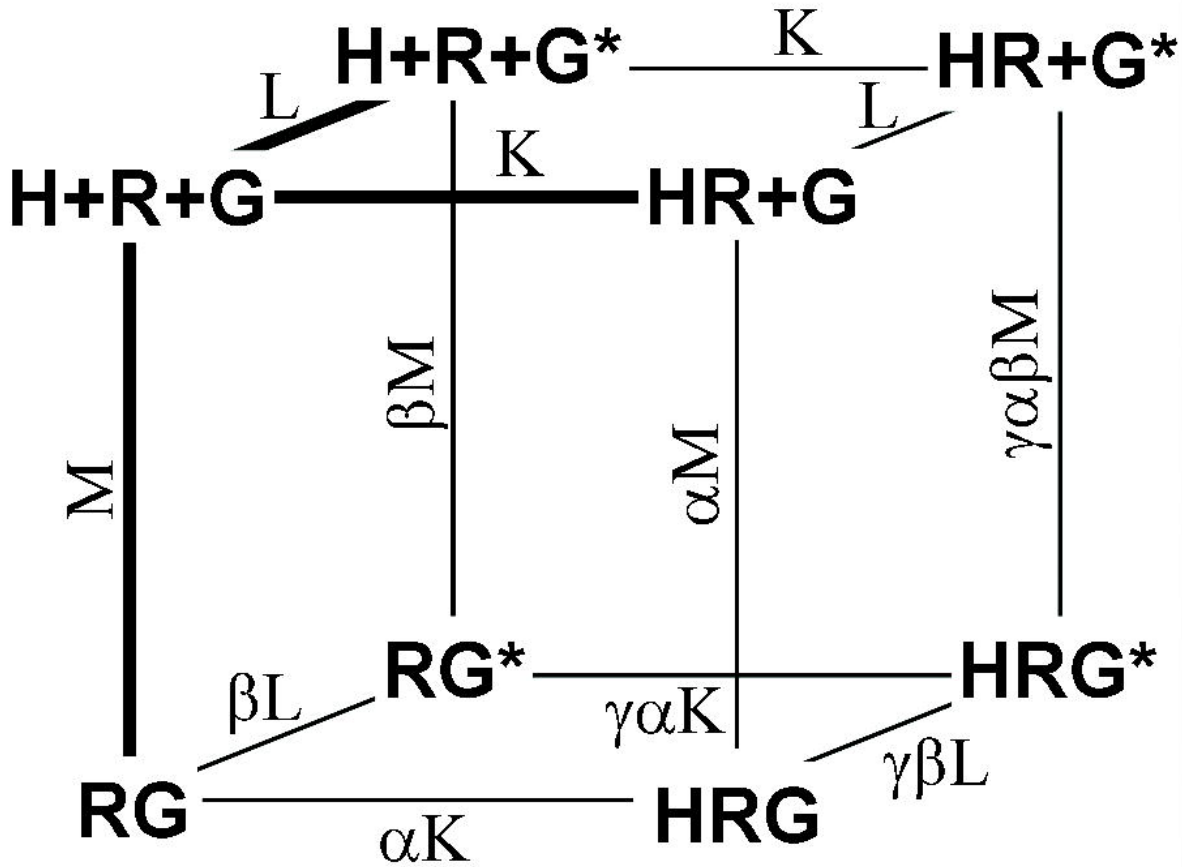
H+R+G*
K
HR+G*
L
L
K
H+R+G
HR+G
M
βM
αM
γαβM
RG*
HRG*
βL
γαK
γβL
RG
αK
HRG

Figure 2

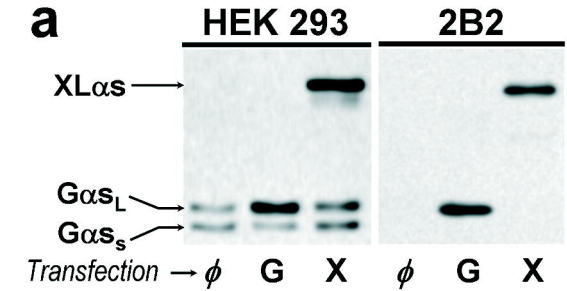
a
HEK 293
2B2
XLαs
GαsL
Gαss
Transfection → ϕ G X ϕ G X

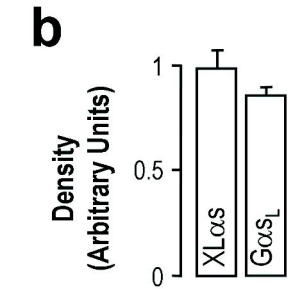
b
Density
(Arbitrary Units)
1
0.5
0
XLαs
GαsL

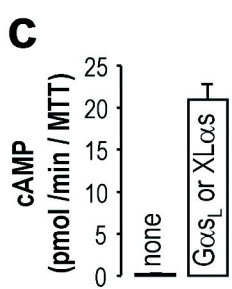
c
cAMP
(pmol /min / MTT)
25
20
15
10
5
0
none
GαsL or XLαs

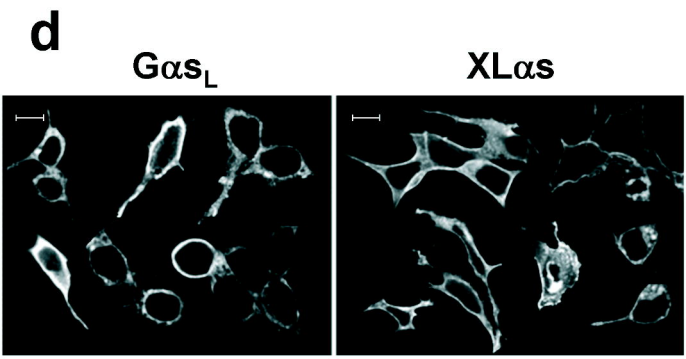
d
GαsL
XLαs

Figure 3

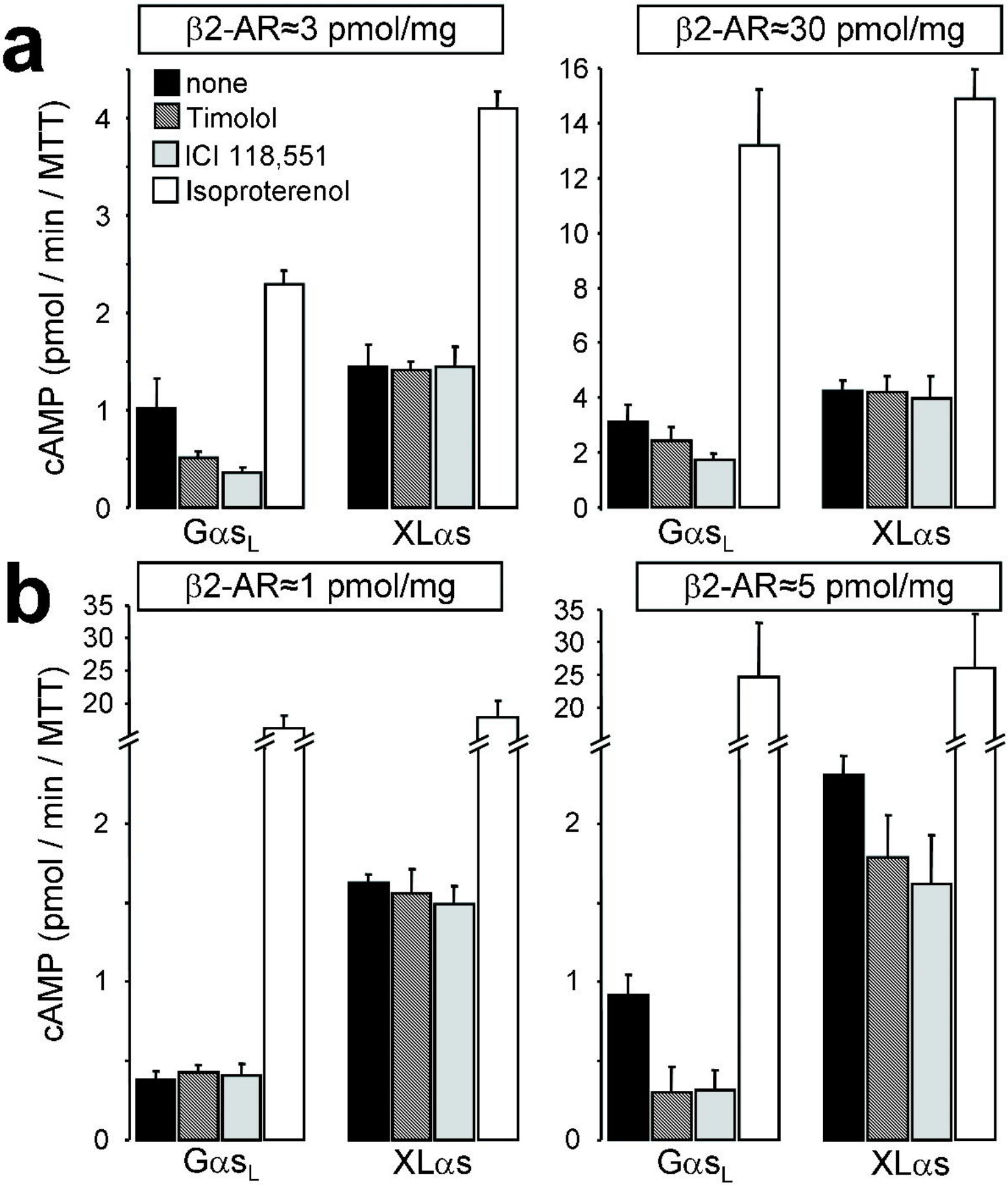
a
β2-AR≈3 pmol/mg
β2-AR≈30 pmol/mg
none
Timolol
ICI 118,551
Isoproterenol
cAMP (pmol / min / MTT)
0
1
2
3
4
6
8
10
12
14
16
GαsL
XLαs
b
β2-AR≈1 pmol/mg
β2-AR≈5 pmol/mg
20
25
30
35

Figure 4

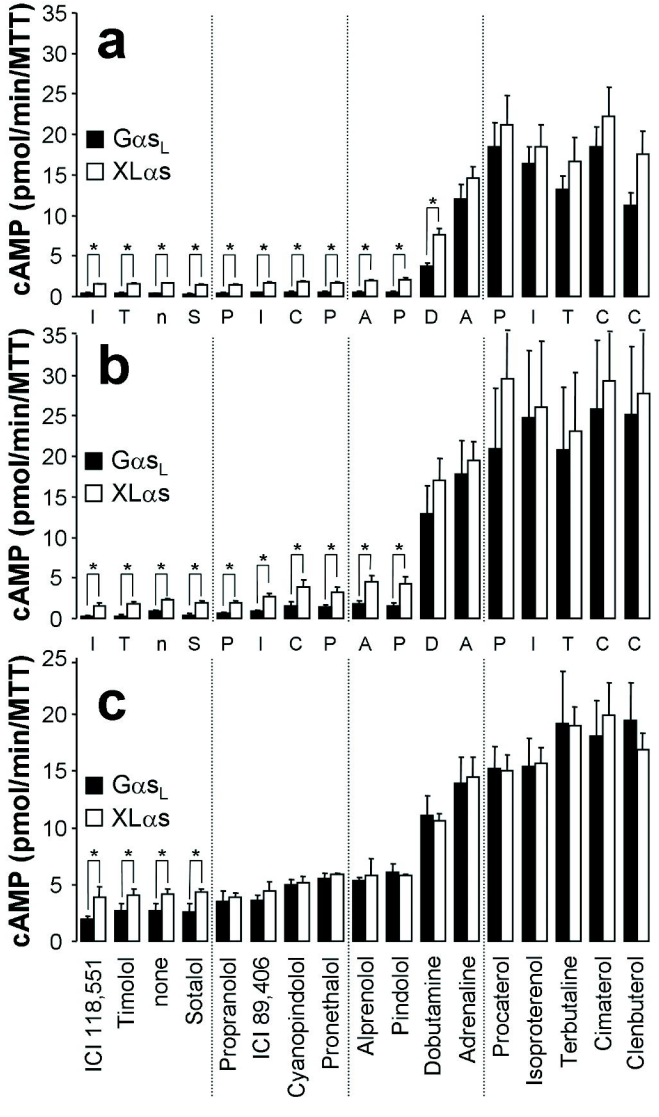
a
b
c
cAMP (pmol/min/MTT)
Gαs$_L$
XLαs
I T n S P I C P A P D A P I T C C
ICI 118,551
Timolol
none
Sotalol
Propranolol
ICI 89,406
Cyanopindolol
Pronethalol
Alprenolol
Pindolol
Dobutamine
Adrenaline
Procaterol
Isoproterenol
Terbutaline
Cimaterol
Clenbuterol

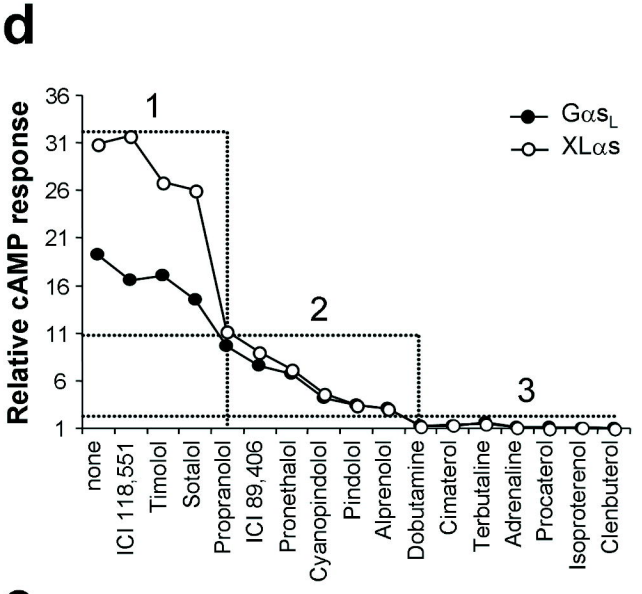
d
Relative cAMP response
Gαs$_L$
XLαs
1
2
3
none
ICI 118,551
Timolol
Sotalol
Propranolol
ICI 89,406
Pronethalol
Cyanopindolol
Pindolol
Alprenolol
Dobutamine
Cimaterol
Terbutaline
Adrenaline
Procaterol
Isoproterenol
Clenbuterol

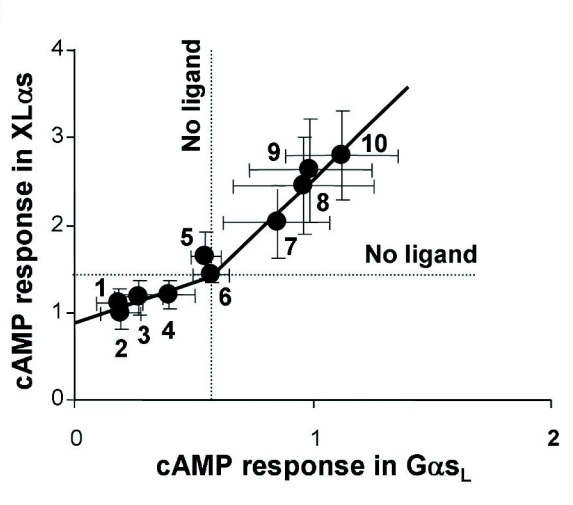
e
cAMP response in XLαs
cAMP response in Gαs$_L$
No ligand
No ligand
1
2
3
4
5
6
7
8
9
10

Figure 5

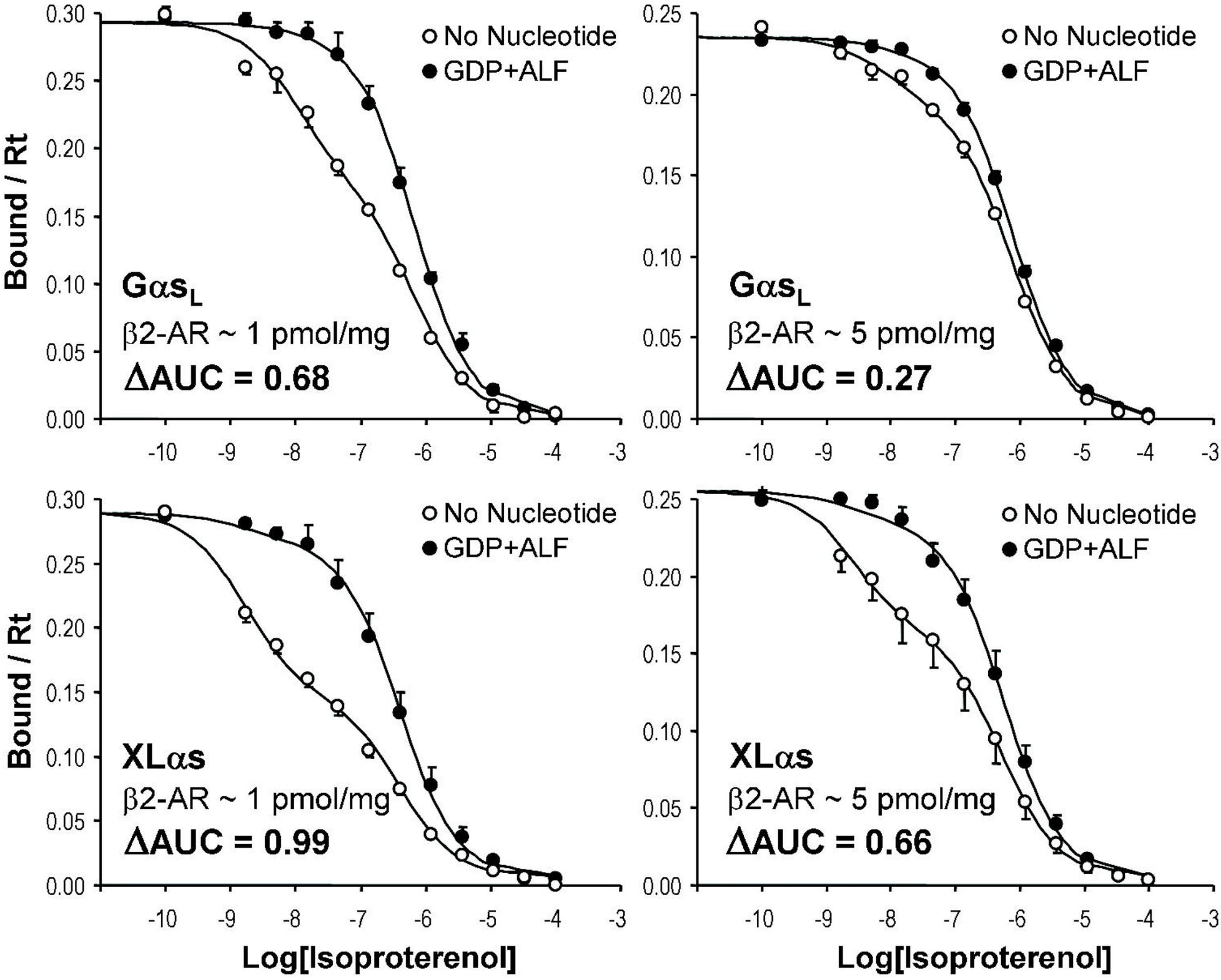
Bound / Rt
No Nucleotide
GDP+ALF
GαsL
β2-AR ~ 1 pmol/mg
ΔAUC = 0.68
GαsL
β2-AR ~ 5 pmol/mg
ΔAUC = 0.27
XLαs
β2-AR ~ 1 pmol/mg
ΔAUC = 0.99
XLαs
β2-AR ~ 5 pmol/mg
ΔAUC = 0.66
Log[Isoproterenol]
Log[Isoproterenol]

Figure 6

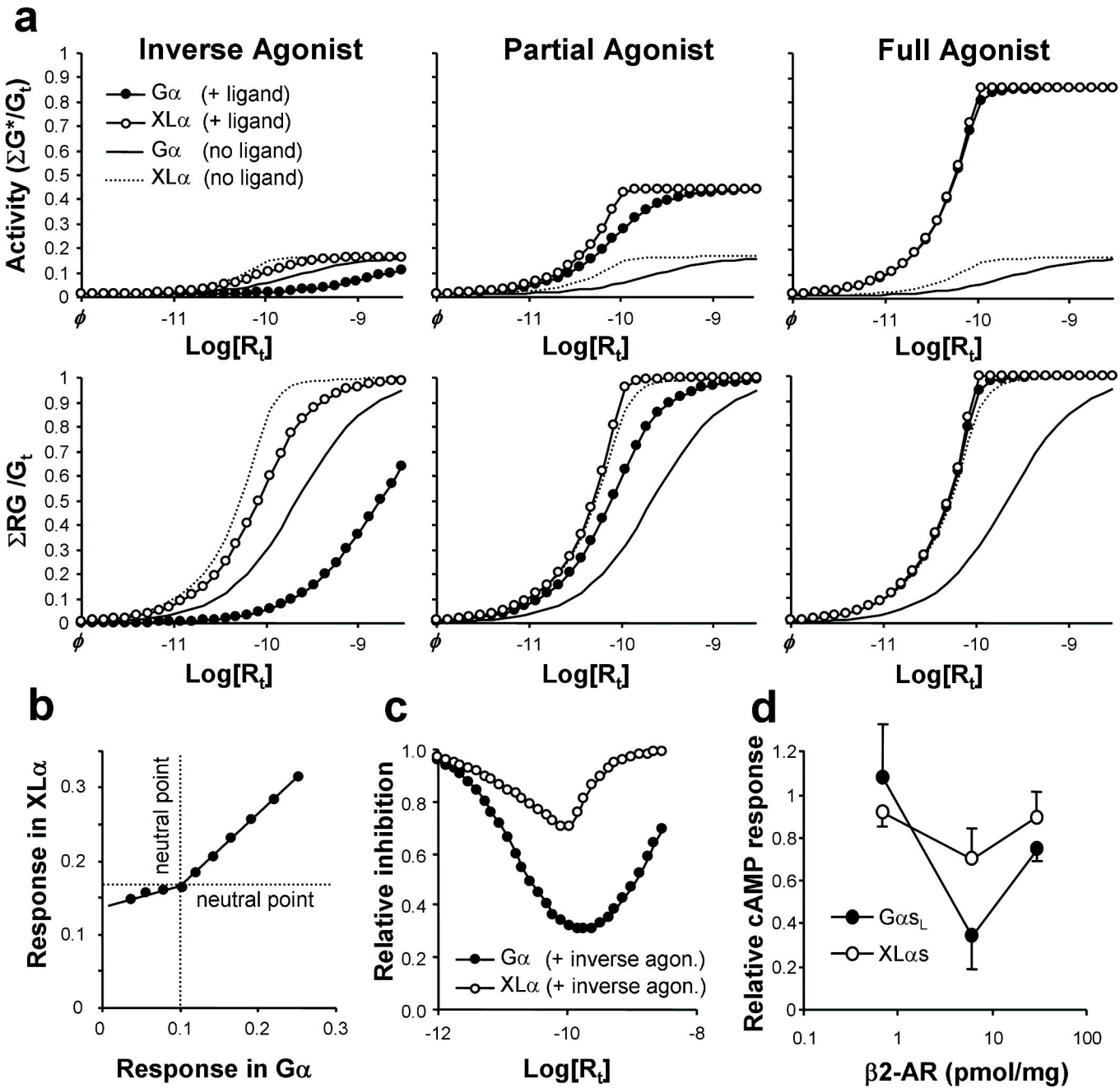
a
Inverse Agonist
Partial Agonist
Full Agonist
Gα (+ ligand)
XLα (+ ligand)
Gα (no ligand)
XLα (no ligand)
Activity (ΣG*/G_t)
ΣRG /G_t
Log[R_t]
b
Response in XLα
Response in Gα
neutral point
c
Relative inhibition
Gα (+ inverse agon.)
XLα (+ inverse agon.)
Log[R_t]
d
Relative cAMP response
Gαs_L
XLαs
β2-AR (pmol/mg)